Effect of repeated loading on bond behavior of GFRP and steel reinforcement embedded in high volume fly ash self-compacting concrete

Waleed awad waryosh[1] [1,2] Civil Engineering Department, Faculty of Engineering, Al-Mustansiriyah University, Baghdad, Iraq.
[1] waleedwaryosh@uomustansiriyah.edu.iq

Bilal rasol[2] [1,2] Civil Engineering Department, Faculty of Engineering, Al-Mustansiriyah University, Baghdad, Iraq.
[2] eama011@uomustansiriyah.edu.iq

ABSTRACT

To reduce the cost of corrosion repairs, the need for corrosion-resistant materials has grown. Glass fiber GFRP is an excellent substitute for reinforcing steel in concrete constructions due to its low cost and good corrosion resistance. However, as the production of cement produces a significant amount of CO2, other options are in high demand. Fly ash is one of the replacements used to partially or fully replace cement in concrete mixtures in order to reduce carbon dioxide emissions. In this study, in addition to the conventional concrete, high-volume fly ash concrete with a 50 % cement replacement was used. Although several research studies have used a pull-out method to conduct an investigation of the bond stress–slip behavior of glass fiber polymer (GFRP) and steel bars implanted in high-volume fly ash concrete, no work has been published on the fatigue bond performance of GFRP or steel bars embedded in high volume fly ash concrete using a hinged beam. This paper discusses the experimental testing of eight hinged beams fabricated in accordance with RILEM standards. With reinforcement bars of 10 mm diameter and bond length 10 times of diameter. The test results show that high volume fly ash concrete exhibited good fatigue bond strength better than conventional concrete for steel bars and GFRP bars.

Keywords: Bond-slip, repeated loading, fly ash, GFRP, High volume fly ash concrete.

1. Introduction

Carbon dioxide emissions and corrosion are the two primary problems with conventional mild steel-reinforced concrete. Corrosion is a serious problem that, if ignored for too long, can result in structural damage[1]. There are around 600,000 bridges in the United States, with 235,000 made of steel-reinforced conventional concrete[1]. About 15% of them are regarded structurally weak due to reinforcing corrosion. The annually direct cost of corrosion, according to the National Association of Corrosion Engineers (NACE), is $8.3 billion [2]. Fiber-reinforced polymer (FRP) bars have been commonly utilized in concrete structures because of their several properties; FRP bars offer excellent material properties, including resistance to corrosion and high tensile strength [3][4]. Using GFRP bars in civil infrastructure is obviously cost-effective in terms of life cycle costs. Reinforcing GFRP bars are 3 times lighter than steel reinforcement bars. Thus, transportation and labor costs are decreased [5].

The second problem is traditional concrete, which is composed of only cement as binder material. In recent years, the cement industry has grown greatly around the world. It is the third-largest emitter of carbon dioxide in the world [6]. Cement is used as a construction material since ancient times, but following World War II, cement usage increased dramatically, with the continued global quantity produced equal to more than half a ton per person per year [6]. Several approaches have been suggested to substitute Portland concrete mixture with a green and sustainable binder. The acceptance of fly ash, a product of coal-burning thermal power plants, is wide[7].

ASTM C618-08 defines fly ash as "the finely separated waste that arises from the burning of ground or powdered coal and is carried by flue gases." The three classes of fly ash products are classes N, F, and C. Chemical compositions differentiate one material from another[8]. Fly ash has been utilized in concrete constructions to replace 15 to 30 percent of the cement[9]. Recent research indicates that replacing cement with a high percentage (up to 75 %) of fly ash can generate concrete that is both durable and strong. High-volume fly ash concrete (HVFAC) is a sustainable and eco-friendly alternative to Portland cement-based concrete. ACI 232.2R defines HVFAC as concrete mixtures with at least 50% fly ash[8]. Fly ash costs $15 to $40 per ton, whereas Portland cement cost $50 to $70 for every ton[10]. HVFAC has been studied extensively in terms of its fresh and hardened characteristics, but little is known about how it behaves structurally[11].

In reinforced concrete, the bond is essential for transmitting stress from the concrete to the reinforcing bar. To ensure a composite action in reinforced concrete members, high bond capacity is essential, and traditional steel bars are usually considered to satisfy bond strength. In contrast to typical steel bars, determining the bond capacity of FRP reinforcement bar is complex. The bond between FRP reinforcement bar and concrete is complex and influenced by a number of parameters. According to previous studies, the most important factors are compressive strength of concrete, bar size, embedment length, geometry, and FRP surface treatment method[12]. Using pullout tests, several experimental investigations have investigated the bond strength of FRP reinforcement bar[4][13] [14][15]. The majority of these were monotonic and uniaxial tests in accordance with the ASTM standard. but few research has been conducted to determining the bond behavior of FRP reinforcing bars under repeated loading, which is necessary to know reinforced concrete structures in a service state under repeated and monotonic loading.

The RILEM Institute [16] suggests the pullout and beam-bond tests as the most commonly recognized and used bond test methods, the real bond behavior of the reinforcement to concrete can only be reflected by the beam-bond test and splice test ,direct pull-out tests on reinforcement bars do not represent the actual bonding conditions.

The primary aim of this study was to investigate the fatigue bond strength of GFRP bars implanted in high-volume fly ash as a sustainable concrete. The study looked at using 50% fly ash instead of Portland cement. Both GFRP and mild steel used 10 mm rebar diameter, with embedment length was 10 times of the bar diameter.

2.Experimental Program

2.1 Test Specimens

Hinged beam testing is one of many approaches for determining the bond behavior of concrete and reinforcement bars. The principle of this test method is to apply flex load to a hinged beam until bond failure occurs for one of the beam or until reinforcement bar itself ruptures [17]. The relative slip between the concrete and the reinforcement bar is recorded during the test. This test method assists in determining the slip or bond capacity of the tested bars by applying the load at the midpoint of the bar in the tension zone. This method was used for this study because the beam test is more representative of actual structural elements and so offers a more accurate estimation of bond strength (especially to flexural members) [18].

A program of testing included eight beam specimens with dimensions of 100 x 200 mm

and a length of 820 mm. The bond length was 10 Ø (varying with bar diameter), while the remaining bars were unbounded. The test beam consists of two RC blocks joined at the bottom by GFRP or steel bar (10mm diameter), that will be used to evaluate the bond strength and steel hinge at the top of the beam.

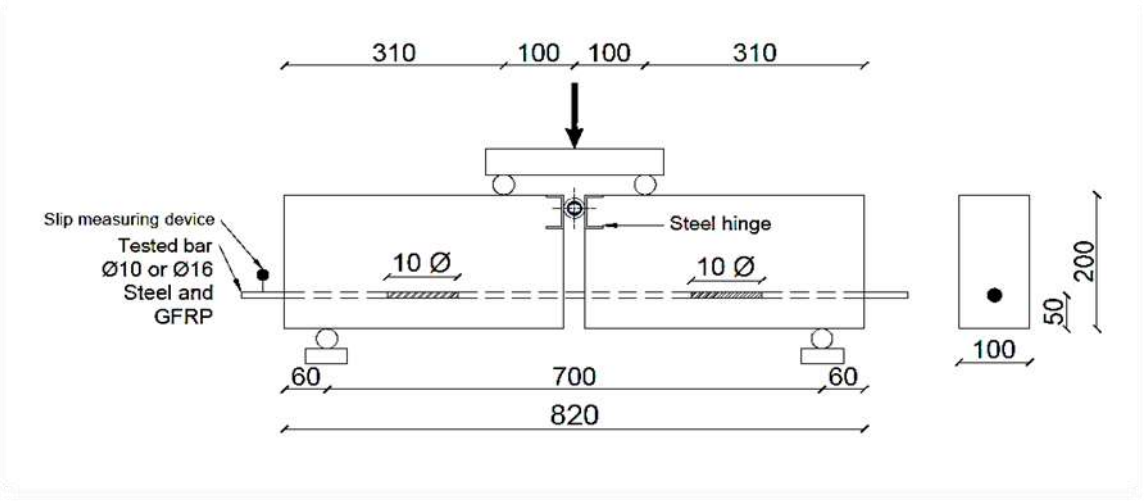

Figure. 1. Geometry of beams[19]

It is necessary to prevent shear cracks of the beam while loading, therefore stirrups with a diameter of 8 mm, and a spacing of 70 mm were utilized to assure the shear resistance of the beam specimen, **Fig. 2.** The distance between the center of the GFRP/steel bars under investigation and the bottom edge of the beam was determined to be constant and equivalent to 50 mm Two 10 mm-diameter reinforcing bars were utilized for the top and the bottom. At the center of the beam's height, there were two steel bars with a 10 mm diameter. The distance between both the centroid of the tested GFRP/steel bars and the bottom surface of the beam was constant and equal to 50 mm.

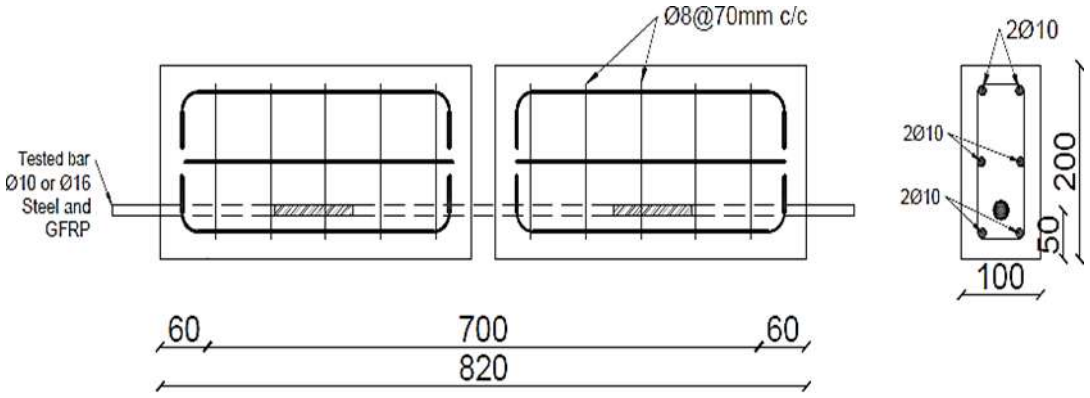

Figure.2. Beam Reinforcement

A notation method by using three symbols was utilized to categorize the specimens that were tested. The notation method is illustrated as follows:

- ❖ The first symbol describes the type of concrete:
- The symbol (NC) refer to the sample is from the normal concrete group.
- The symbol (F50) refer to that specimen from a high-volume ash group. It is subscripted by the number (50), which represents of cement replacement by fly ash.
- ❖ The second symbols describe the type of

Specimen	Concrete Type	Rebar Type	Type of loading
NC-St10M	Normal Concrete	Steel	monotonic
NC-St10R			repeated
NC-GF10M		Glass Fiber	monotonic
NC-GF10R			repeated
FA50St10M	High volume fly ash concrete	Steel	monotonic
FA50St10R			repeated
FA50GF10M		Glass Fiber	monotonic
FA50GF10R			repeated

investigated bar:

- The symbol (St) refer to the sample from Steel group and (G) refer to the sample from Glass Fiber group. It is subscripted by the number (10), which denote bar diameter in denotes.

❖ The third symbol describe the type of loading:

- The symbol (M) refer to monotonic loading.
- The symbol (R) refer to repeated loading

Table 1. Specimen details.

2.2. Material Characteristics

2.2.1Steel Bars

In this work, three reinforcement steel bars with different diameters of 8, 10, and 16 mm were utilized.

Testing of these bars was conducted at the College of Engineering, Al-Mustansiriya University the test results are presented in Table (2). The results of the testing for these bars were in compliance with ASTM A615/A615M [20]

Table .2. Tension results of Steel bars.

Nominal Diameter (mm)	Yield Stress (MPa)	Ultimate Strength (MP)	Total elongation (%)
8	517	654	10
10	580	645	9
16	522	661	9

2.2.2GFRB Bars

In this work, two diameters of the GFRP rebar were employed as longitudinal test bars to investigate bond behavior with concrete. The mechanical properties of GFRB bars are drawn in the table (3).

Table .3. Properties of GFRP bar

Diameter Bar (mm)	Ultimate tensile Load (KN)	Guaranteed Tensile strength (MPa)	Modules of elasticity (Gpa)
10	59	827	46
16	143	724	46

2.2.3Cement

Portland Limestone Cement (Karesta Company), symbol CEM II/ A-L, was used in this investigation. The physical and chemical properties of cement are shown in Tables (4). This cement's test results meet the requirements of IQ.S. 5:2019[21] .

2.2.4Fly ash

This research uses Class F fly ash provided by " EUROBUILD " construction chemicals company. The X-Ray Fuorescence (XRF) testing was performed according to BS EN 196-2-2013, and the findings are shown in Table .4.

Table .4. Chemical and physical properties of cementitious materials.

Properties	Unit	Cement	Limitation IQ.S. NO.5:2019 [21]	Fly Ash	Limits of ASTM C 618-03[22]
SiO2	%	18.14		47.67	Total ≥ 70%
Al2O3		6.71		27.73	
Fe2O3		2.9		18.42	
Cao		60.74		5.11	
MgO		1.28	< 5	2.65	
SO3		2.09	< 2.8	3.71	≤5
Na2O		…		…	
K2O		….		…	
Na2O		…..		…	
Loss in ignition		2.25	< 4	3.71	≤6
Fineness(Blaine)	Cm2/gm	4678	> 2800	…	
C3S		…		…	
C2S		…		…	
C3A		12.88		42.38	
C4AF		…		…	
Vicat set time, initial	minutes	125	≥45	…	
Vicat set time, final	hours	3.5	≤ 10	…	
Specific gravity		…		2.2	

2.2.1 Fine Aggregate

This study used natural sand as fine aggregate for concrete mixtures; it includes rounded particles with a smooth texture and a maximum particle size of 4.75mm. The limits of IOS No. 45/1984 are observed during sieve analysis.[23].

2.2.5 Coarse Aggregate

The concrete samples were cast using crushed gravel with a maximum particle size of 12 mm. Physical and chemical properties are examined in compliance with IOS No. 45/1984 restrictions.[23].

2.2.6 Limestone Powder

The fine limestone powder is extremely good in preventing high temperatures generation, enhancing fluidity and cohesiveness, enhancing segregation resistance, and increasing the quantity of fine powder in the mixes. [24].

2.2.8 Superplasticizers (Sika Viscocrete-5930)

It is a highly plasticizing admixture of the third generation. Its basis is an aqueous solution of poly-carboxylate that has been modified. The superplasticizers (Sika Viscocrete-5930) used in this investigation exceed the ASTM standard requirements for classes G and F (ASTM C494/C494M, 2015).

2.3 Concrete mixes

In this study, two mixes (high volume fly ash concrete and conventional concrete) were poured to obtain a compressive strength of 30MPa for 150*150*150 mm cubes after 28 days. Conventional concrete slump testing done is in accordance with (ASTM) C143. [25]. High volume fly ash concrete is classified as self-compacting concrete if its fresh properties correspond to the EFNARC criteria. [26].

Table .5. details mixes

Mix	Cement (kg/m3)	Fly ash (kg/m3)	Limestone (kg/m3)	Fine aggregate (kg/m3)	Coarse aggregate (kg/m3)	Water (kg/m3)	Superplasticizer (l/m3)
Normal concrete[27]	400	…….	…….	600	1200	180	…….
High volume fly ash concrete[28]	200	200	100	840	800	170	5.4

Table .6. test results of fresh high-volume fly ash self-compacting concrete.

Test	Property	Unit	Test results	Range[26]
Slump flow	Filling ability	mm	750	650-800
T50		sec	3	2-5
V-funnel	Segregation resistance	sec	9	6-12
L-box	Pass ability	%	0.9	0.8-1

Table .7. Mechanical properties of hardened concrete

Mix	Compressive Strength		Rupture Modulus (fr) (mpa) [29]	Splitting Tensile Strength (fct) (mpa) [30]	Elasticity Modulus (Ec) (GPa) [31]
	fcu (mpa) [32]	f′c (mpa) [33]			
Conventional concrete	32.5	28.3	4	2.98	24.2
High volume fly ash concrete	36	30.24	4.5	3.5	23

2.4 Test Setup And Test Measurements

The devices have been used to evaluate the bond behavior of tested beams; these devices are used to monitor the values of load or relative slip between both the tested bar (steel/GFRB) and surrounding concrete at each loading stage. All specimens of beams were examined with hydraulic ELE flexural testing equipment at The Building of Material Laboratory College of Engineering, Mustansiriya University.

The beam samples are placed under a two-point load on the testing machine, balanced according to the appropriate distance between the support point loads, as well as the dial gauges are adjusted to their respective locations, as illustrated **Fig .3.**

(a) ELE Machine Test

(b) Test setup

Figure.3. Testing Setup of the Beam Specimen under test machine.

3. Analysis of Test Results

3.1 Bond Stress Results

The ultimate pull-out force (Pu) in the tested bar was determined based on maximum load (Fmax).

$$Pu = \frac{Fmax.a}{2.b} \quad \text{..... (1)}$$

Where Pu is the pull-out force applied to the tested bar (KN), F is the maximum applied load (KN), an is the shear span (mm), and ;(b) is the lever arm from the center of the steel hinge to the center of the tested bar (mm).

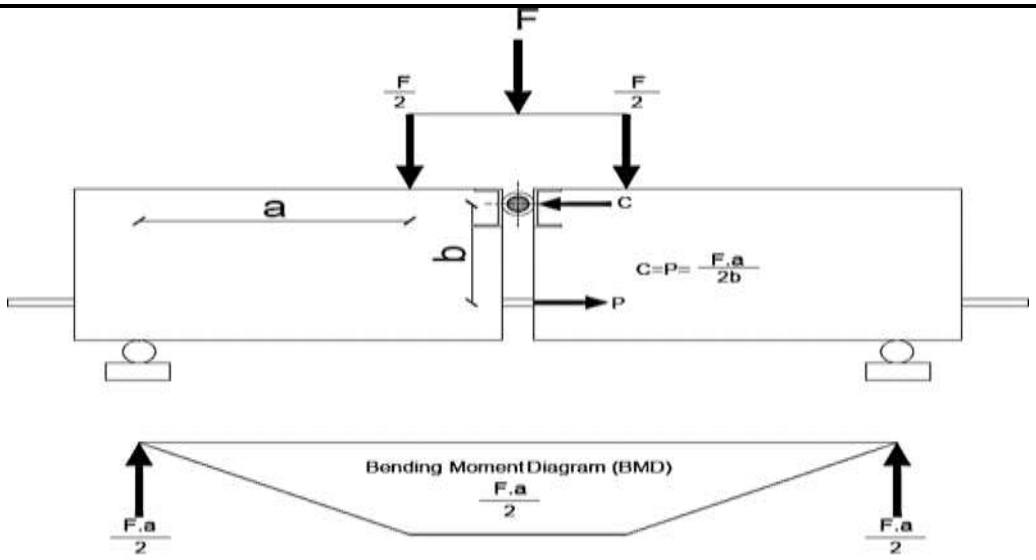

Figure .4. pull-out force calculation RILEM concept in the deformed bar.

The ultimate bond stress of the bar (**τ**u), defined as the average shear stress along the bonded length, was then calculated using equation (2).

$$\tau u = \frac{Pu}{\pi.\emptyset.Lb} \text{ ..... (2)}$$

Where Pu represents the ultimate pull-out force, Ø represents the nominal bar diameter, and Lb represents the bonded length.

3.2 Failure mechanism

In this investigation, the mechanism of failure was observed for every hinge beam specimen. The majority of specimens failed by a pull-out mode, as illustrated in **Fig. 5 to 8**, with the exception of beams reinforced with steel bars (FA50St10M) and specimens reinforced with GFRP bar (FA50GF10M), which failed by bar rupture, as illustrated in **Fig. 7 (b)** and **8 (b)**. After testing, some hinge beams were split in half to determine the mechanism of failure, the external layer of the GFRP reinforcing bar and adjacent concrete within the implanted part were investigated for information relating to bond concepts. For glass-fiber specimens, some abrasions were observed on the outer layer and strip of the sand-coated layer, also through observations, it was observed the fiber was damaged, as shown in **Fig.9.** It must be mentioned that the specimens (FA50St10M) and (FA50GF10M) failed due to rupture bar under monotonic loading. while comparable specimens (FA50ST10M) and (FA50GF10M) failed due to a pull-out failure by repeated loading, as shown in **Fig. 7** and **8.**

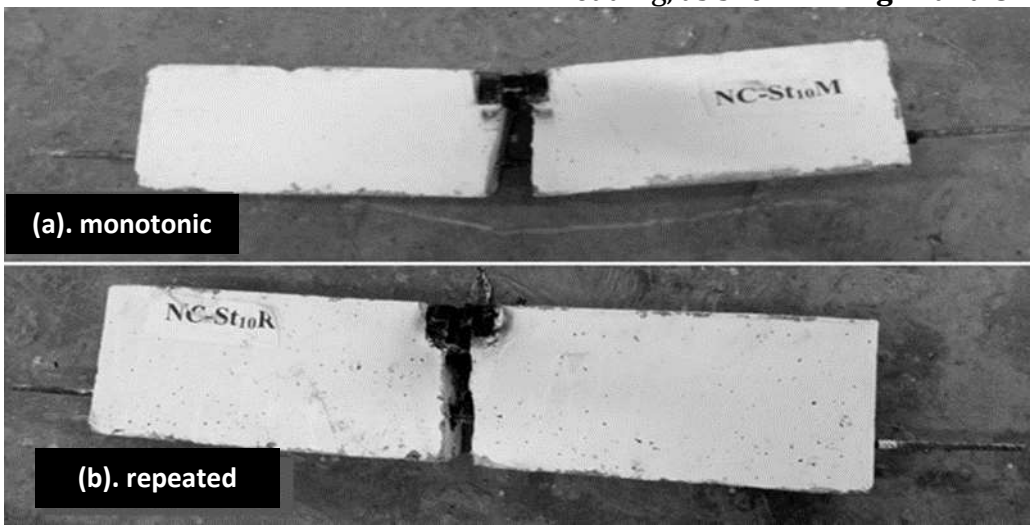

Figure .5. (a) pull-out failure of the steel-reinforced specimen (monotonic loading).
(b) pull-out failure of the steel-reinforced specimen (repeated loading).

Figure.6. (a) pull-out failure of GFRP-reinforced specimen (monotonic loading)
(b) pull-out failure of GFRP-reinforced specimen (repeated loading)

Figure .7. (a) pull-out failure of the steel-reinforced specimen (monotonic loading)
(b) pull-out failure of the steel-reinforced specimen (repeated loading)

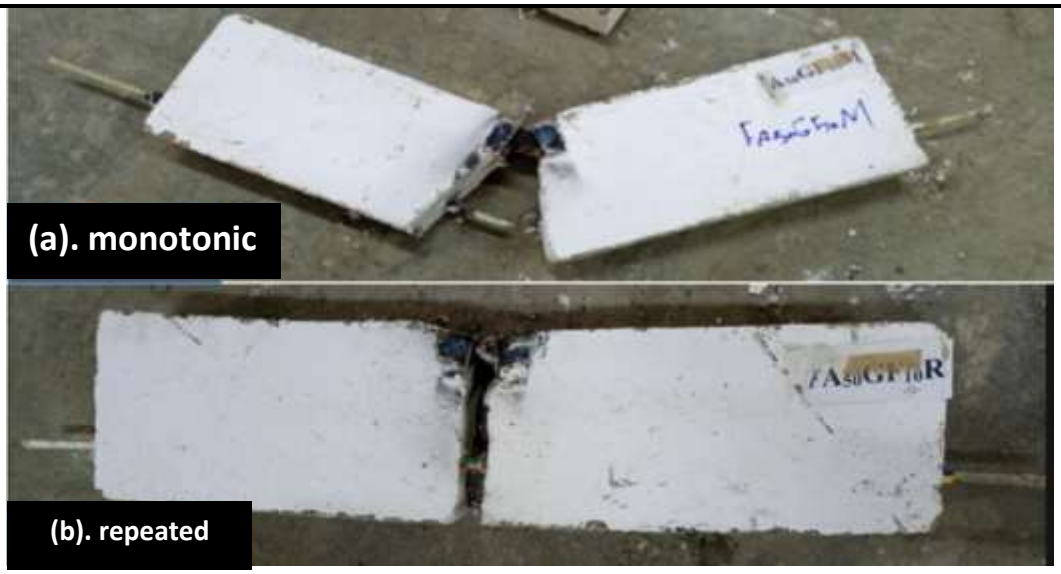

Figure.8. (a) Bar rupture failure of GFRP-reinforced specimen (monotonic loading)
(b) pull-out failure of GFRP-reinforced specimen (repeated loading)

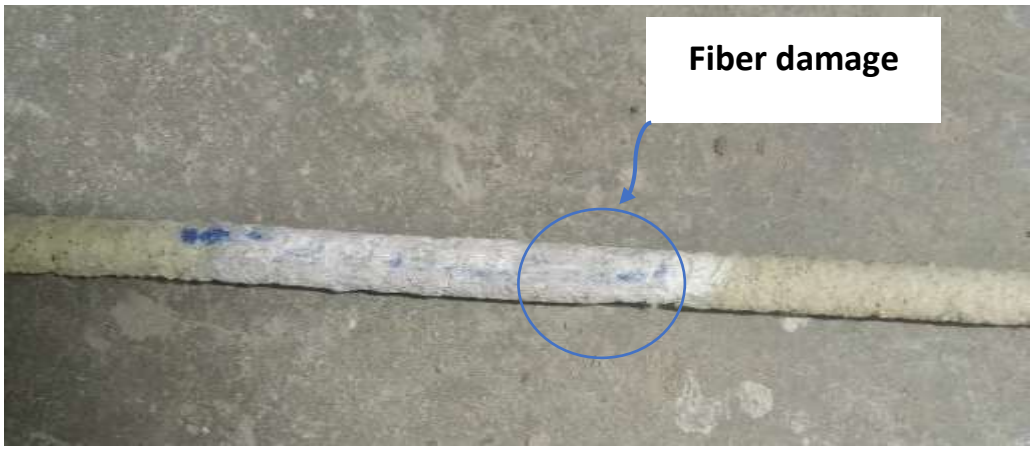

Figure.9. abrasion outer layer and damage fibers within the embedded length of GFRP bar.

3.3 Effect of repeated loading on ultimate bond strength

Beam samples tested under monotonic load are considered reference beams for similar beams tested under cyclic loadings as a percentage of their corresponding control monotonic load beams. In general, high volume fly ash concrete showed fatigue resistance more than conventional concrete, also GFRP bars exhibited fatigue resistance slightly more than steel bars. **Fig.10.** and **Fig.11.** explained the reduction in ultimate bond strength for a beam under repeated loading compared to similar beams after repeated loading. For conventional concrete, steel bar subjected to repeated loading exhibited ultimate bond strength 7 % less than similar beams under monotonic loading, with the same pattern GFRP tested bar exhibited 3.7 % reduction percentage due to fatigue loading. Steel bar embedded in high volume fly ash concrete subjected to repeated loading had an ultimate bond strength 2.2 % lower than corresponding beams under monotonic loading, whereas GFRP tested bar showed a 1.6 % drop percentage according to fatigue loading.

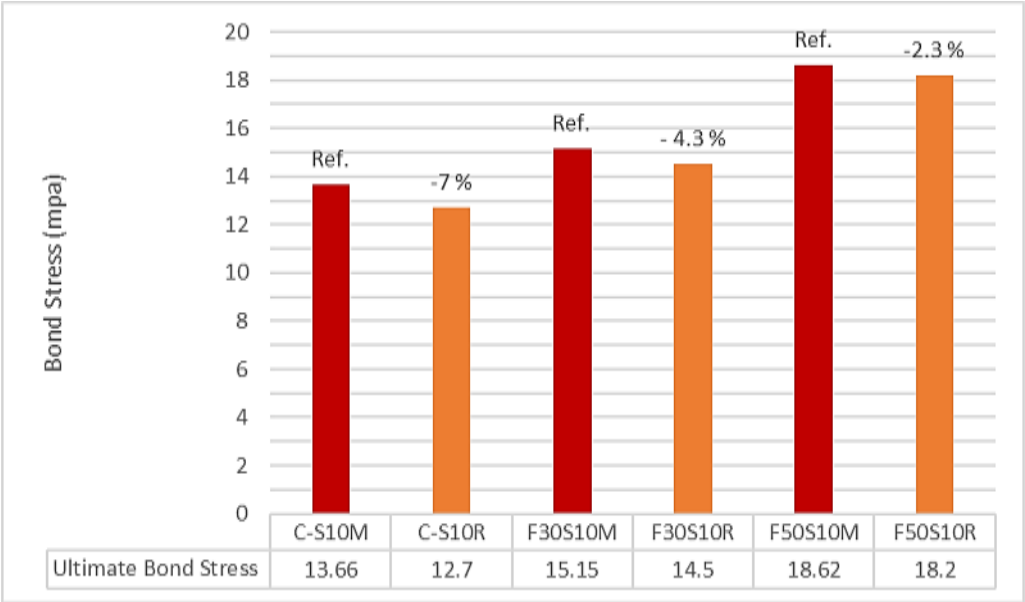

Figure .10. Comparison ultimate bond stress of steel bars under repeated and monotonic loading.

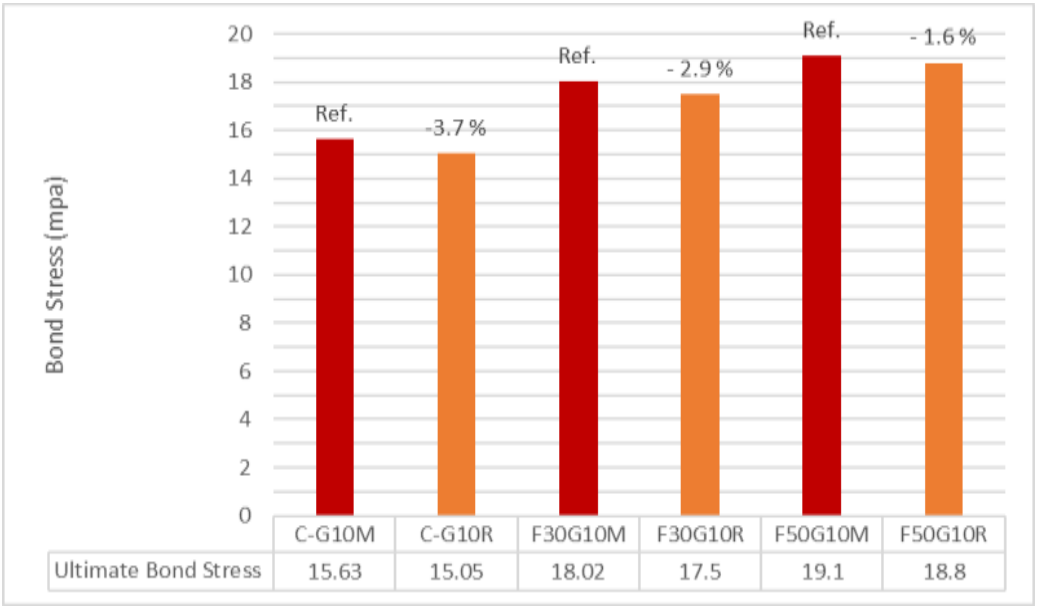

Figure .11. Comparison ultimate bond stress of GFRP bar under repeated monotonic loading.

3.4 Bond stress – slip relationship

Figure 5 to 7 illustrates the bond stress–slip relation of steel-reinforced hinged beams under monotonic and repeated loading. For monotonic specimen, bond stress versus slip relationships is shown according to the type of loading in order to investigate the effect of fatigue loading on the bond behavior of GFRP and steel reinforcing bar embedded in conventional concrete and high-volume fly ash concrete. The typical bond stress–slip behavior is characterized by high initial bond stress without a noticeable slip in both GFRP and steel bars due to good chemical interaction between both the bar surface and adjacent concrete. After the chemical attraction has been lost, bond stress continues to develop with a tiny slip increase until it reaches its maximum. At this point, friction and bearing dominate to resist the pull-out force for steel reinforcing bars, but only friction resistance dominates the response for GFRP reinforced hinged beams.

This trend was observed for all hinged beams reinforced with GFRP except for two specimens FA50GF10M and FA50St10M, where the curve suddenly stops due to rupture bar failure before bond failure. For repeated specimens, also the chemical bond is effective in the first cycles of fatigue loading, then an increase in slip is observed. Specimens of high volume fly ash concrete exhibited closeness to monotonic curve for similar beam, this related that bond strength of high volume fly ash concrete not much affected by cyclic loads.

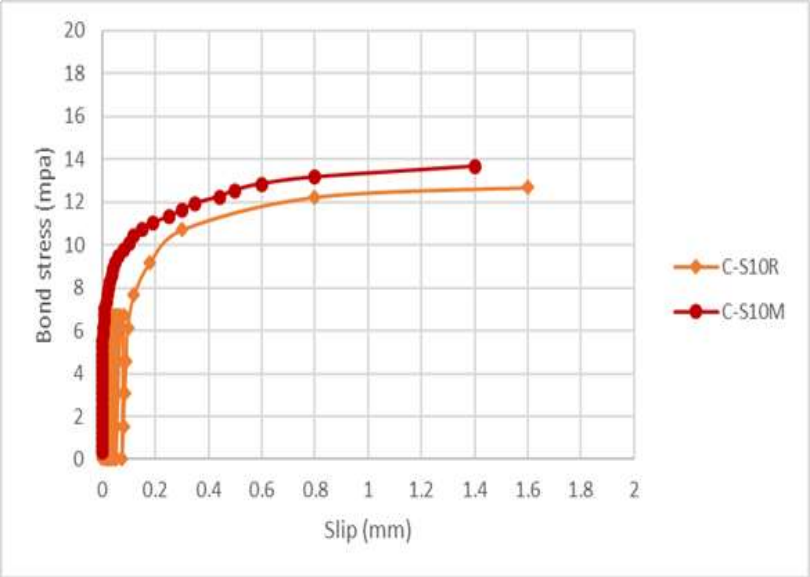

Figure .12. Bond-slip relation of steel bars embedded in conventional concrete according to monotonic and repeated loading.

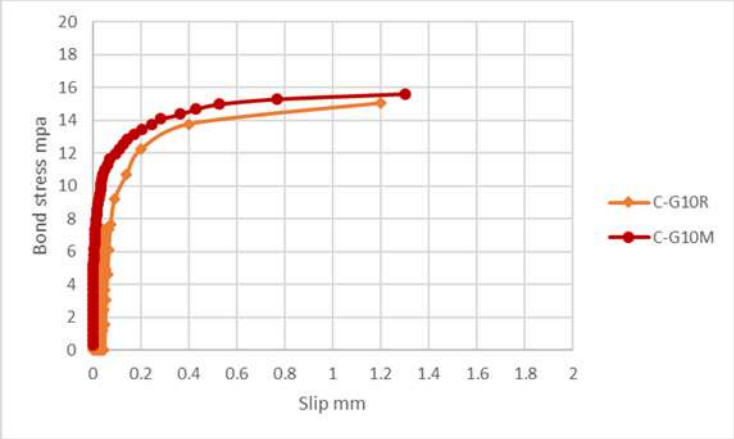

Figure.13. Bond-slip relation of GFRP bars embedded in conventional concrete according to monotonic and repeated loading.

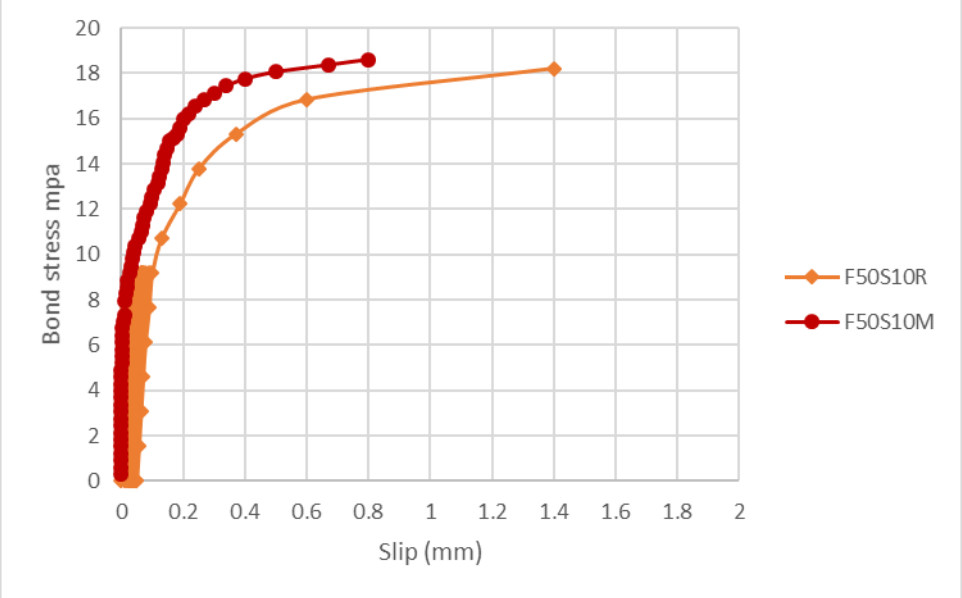

Figure.14. Bond-slip relation of steel bars embedded in high volume fly ash concrete according to monotonic and repeated loading.

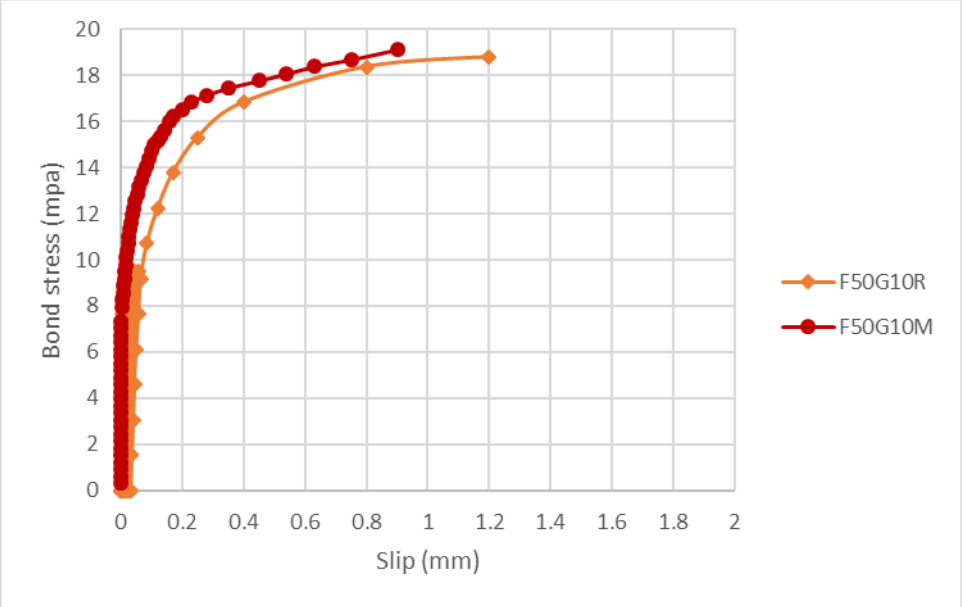

Figure.15. Bond-slip relation of GFRP bars embedded in high volume fly ash concrete according to monotonic and repeated loading.

4. Conclusions

In this study, the fatigue bond strength behavior of GFRP and steel rebar was investigated. The specimens were subjected to 10 cycles until 50% of the failure load for a similar beam under monotonic loading was reached, and finally monotonic loading until specimen failure. The conclusions are listed below:

- For steel and GFRP bars, high volume fly ash concrete specimens exhibited fatigue resistance more than specimens of conventional concrete.
- For all specimens, bond strength at failure after cyclic loading decreases at different rates (7 % to 1.6%) when compared with those under monotonic loading. This was produced by repetitive stress on the bond surface, which reduced the adhesion capacity between both the concrete and the GFRP reinforcing bar. Therefore, bonding in

designs should be investigated for fatigue behavior of the flexural members.

- High volume fly ash concrete and GFRP bar were shown to have adequate bond performance under repeated loading conditions, such as vehicle traffic; hence, it may be applied in the construction of infrastructure subjected to fatigue.
- Finally, as the results indicated in this that GFRP bars are considered good alternative to steel reinforcement in terms of resisting repetitive loads, an example of that is the vehicle movement found on reinforced concrete bridges.

References

[1] R. J. Kessler and R. G. Powers, Corrosion of Epoxy Coated Rebar, Keys Segmental Bridges, Monroe County. Florida Department of Transportation, Materials Office, 1988.

[2] G. H. Koch, M. P. H. Brongers, N. G. Thompson, Y. P. Virmani, and J. H. Payer, "Corrosion cost and preventive strategies in the United States," United States. Federal Highway Administration, 2013.

[3] A. Khalifa, W. J. Gold, A. Nanni, and A. A. MI, "Contribution of externally bonded FRP to shear capacity of RC flexural members," J. Compos. Constr., vol. 2, no. 4, pp. 195–202, 1998.

[4] Z. Achillides and K. Pilakoutas, "Bond behavior of fiber reinforced polymer bars under direct pullout conditions," J. Compos. Constr., vol. 8, no. 2, pp. 173–181, 2004.

[5] S. Skapa, "Investment characteristics of natural monopoly companies," J. Compet., vol. 4, no. 1, 2012.

[6] R. M. Andrew, "Global CO 2 emissions from cement production," Earth Syst. Sci. Data, vol. 10, no. 1, pp. 195–217, 2018, [Online]. Available: https://doi.org/10.5194/essd-10-195-2018.%0AAnon, 1985. Fly ash. Concr. Constr. - World Concr. 30 (4).

[7] A. Bilodeau and V. M. Malhotra, "High-volume fly ash system: concrete solution for sustainable development," Mater. J., vol. 97, no. 1, pp. 41–48, 2000.

[8] A. C. I. C. 232, "232.2 R-18: Report for the Use of Fly Ash in Concrete," 2018.

[9] E. E. Berry, R. T. Hemmings, M.-H. Zhang, B. J. Cornelius, and D. M. Golden, "Hydration in high-volume fly ash concrete binders," Mater. J., vol. 91, no. 4, pp. 382–389, 1994, [Online]. Available: https://doi.org/10.14359/4054.

[10] E. Yuuml; ksel, "The effect of cure conditions and temperature changes on the compressive strength of normal and fly ash-added concretes," Int. J. Phys. Sci., vol. 5, no. 17, pp. 2598–2604, 2010.

[11] M. Arezoumandi, T. J. Looney, and J. S. Volz, "Effect of fly ash replacement level on the bond strength of reinforcing steel in concrete beams," J. Clean. Prod., vol. 87, pp. 745–751, 2015.

[12] E. Cosenza, G. Manfredi, and R. Realfonzo, "Behavior and modeling of bond of FRP rebars to concrete," J. Compos. Constr., vol. 1, no. 2, pp. 40–51, 1997.

[13] E. Cosenza, G. Manfredi, and R. Realfonzo, "Development length of FRP straight rebars," Compos. Part B Eng., vol. 33, no. 7, pp. 493–504, 2002.

[14] W. Xue, Q. Zheng, Y. Yang, and Z. Fang, "Bond behavior of sand-coated deformed glass fiber reinforced polymer rebars," J. Reinf. Plast. Compos., vol. 33, no. 10, pp. 895–910, 2014.

[15] M. Baena, L. Torres, A. Turon, and C. Barris, "Experimental study of bond behaviour between concrete and FRP bars using a pull-out test," Compos. Part B Eng., vol. 40, no. 8, pp. 784–797, 2009.

[16] T. C. RILEM, "RC 6: Bond test reinforcing steel, 2, pull-out test," London E FN SPON, 1983.

[17] M. Seis and A. Beycioğlu, "Bond performance of basalt fiber-reinforced polymer bars in conventional Portland cement concrete: A relative comparison with steel rebar using the hinged beam approach," Sci. Eng. Compos. Mater., vol. 24, no. 6, pp. 909–918, 2017.

[18] I. Pop, G. De Schutter, P. Desnerck, and T. Onet, "Bond between powder type self-compacting concrete and steel reinforcement," Constr. Build. Mater., vol.

41, pp. 824–833, 2013.
[19] D. Szczech and R. Kotynia, "Beam bond tests of GFRP and steel reinforcement to concrete," Arch. Civ. Eng., vol. 64, no. 4/II, 2018.
[20] S. ASTM, "Standard specification for deformed and plain carbon-steel bars for concrete reinforcement," ASTM A615/A615M-09b, 2009.
[21] I. S. Specification, "No. 5/2019, Portland Cement," Cent. Organ. Stand. Qual. Control (COSQC), Baghdad, Iraq, 2019.
[22] A. Standard, "Standard specification for coal fly ash and raw or calcined natural pozzolan for use in concrete," ASTM Stand. C, vol. 618, 2012.
[23] N. 45 Iraqi Specification, "Aggregate from Natural Sources for Concrete and Construction." Ministry of Planning, Central Organization for Standardization and Quality …, 1984.
[24] L. O. Larsen and V. V Naruts, "Self-compacting concrete with limestone powder for transport infrastructure.," Mag. Civ. Eng., no. 8, 2016.
[25] C. ASTM, "Standard test method for slump of hydraulic-cement concrete," ASTM Int. West Conshohocken, PA, 2012.
[26] F. EFNARC, "Specification and guidelines for self-compacting concrete," Eur. Fed. Spec. Constr. Chem. Concr. Syst., 2002.
[27] M. H. Mohammed, "Reinforced Concrete Strengthening by Using Geotextile Reinforcement for Foundations and Slabs," Master Sci. Civ. Eng. Civ. Eng. Dep. Fac. Eng. Al-Mustansiriayah Univ., 2017.
[28] A. A. Taha, "Performance of high-volume fly ash self-compacting concrete exposed to external sulfate attack," 2019.
[29] C. ASTM, "Standard test method for flexural strength of concrete (using simple beam with third-point loading)," in American society for testing and materials, 2010, vol. 100, pp. 12959–19428.
[30] A. S. for T. and M. (ASTM), "Standard Test Method for Splitting Tensile Strength of Cylindrical Concrete Specimens.(ASTM C496/C496M-11)," 2011.
[31] A. Standard, "Standard test method for static modulus of elasticity and poisson's ratio of concrete in compression," ASTM Stand. C, vol. 469, 2010.
[32] B. S. Standard, "Method for determination of compressive strength of concrete cubes concrete specimens," BS, vol. 116, p. 1983, 1881.
[33] A. I. C. C. on C. and C. Aggregates, Standard test method for compressive strength of cylindrical concrete specimens. ASTM international, 2014.